Nanoscale

PAPER

View Article Online
View Journal

Cite this: DOI: 10.1039/c6nr09408b

Defining the copper binding aptamotif and aptamer integrated recovery platform (AIRP)†

Simranjeet Singh Sekhon,[a] Sang-Hee Lee,[a] Kyeong-Ah Lee,[a] Jiho Min,[b] Byung-Tae Lee,[c] Kyoung-Woong Kim,[c] Ji-Young Ahn*[a] and Yang-Hoon Kim*[a]

Received 5th December 2016,
Accepted 29th January 2017

DOI: 10.1039/c6nr09408b

rsc.li/nanoscale

The potential copper binding sites in aptamers have been predicted on the basis of secondary structures and the binding affinity of aptamers with copper. Out of the 4 aptamers (Cu-A1 to Cu-A4) selected by SELEX and examined in the present study, the Cu-A2 aptamer shows the highest binding affinity to copper with the lowest K_D value of 1.83×10^{-11} M. In order to confirm the binding of copper to the proposed region, the binding affinity was experimentally validated using mutation and deletion analysis. We have confirmed that the high G–C pairing patterns and short stem-interval distance play important roles in copper binding. Aptamer specificity was also verified against diverse heavy metals. We also demonstrate an Aptamer Integrated Recovery Platform (AIRP) to recover copper from acidic mine drainage. AIRP can be easily regenerated at least 20 times without significant deterioration of the retrieval performance. To the best of our knowledge, AIRP is the first demonstration of copper specific recovery using aptamers. This can be scaled up and would have diverse applications in metal contaminated water treatment, recovery and as a potential biosensor for environmental analysis, monitoring, and risk assessment.

Introduction

Copper (Cu) is one of the best electrical conductors among all the raw metals. Copper plays a more important role in renewable energy generation than in conventional thermal power plants.[1] It is also being widely seen as a leading economic indicator. Generally, copper is extracted from ores rich in copper sulfides, which is mined at present from the large open pits in South America, North America, Asia, Africa and Middle East.[2] Increasing industrialization and urbanization worldwide have substantially ravaged our environment through the discharge of industrial and domestic wastes. These waste waters are frequently laden with toxic heavy metals such as copper in which significant amounts are deposited into the natural aquatic and terrestrial ecosystems.[3]

In particular, the presence of copper in drinking water poses serious human health hazards because of its toxicity and tendency to bioaccumulate.[4] For humans, poisoning by copper can result in severe dysfunctions of the kidney, reproductive system, liver, brain and central nervous system.[5–7] Since the environmental pollution caused by copper contamination and toxicity has received much concern, it has triggered numerous studies focusing on its removal and reduction.[8–10] The US EPA indicates copper as a priority pollutant and toxic at concentrations higher than 100 ppm, whereas EC tolerance for copper concentration in water intended for human consumption is 2 ppm.[11] Traditional methods including ion exchange, electrolytical or chemical precipitation, and absorption on activated carbon, reverse osmosis, or solvent extraction have also been used for copper removal, though not applicable in low-concentration solutions.[12,13] However, these methods only allow removal of copper which is ultimately discarded as sludge and does not permit the reuse and recovery of copper, resulting in a waste of raw materials. Moreover, current methods consist of a series of complicated processes such as dissolution of the scrap in solutions, filtering off insoluble constituents, concentrations of filtrates, addition of precipitants, and drying and calcinations of precipitates.[9]

Considerable research work has recently been reported on the use of aptamers in advanced diagnostic as well as in applied industrial fields.[7,14] Aptamers are a new class of synthetic materials with applications over a wide range of fields. Aptamers are short single-stranded (ss) DNA or RNA oligonucleotides that can bind to their targets with high affinity and specificity because of their ability to adopt sequence-dependent 3-dimensional folds in solution.[15] Recently, aptamers are

[a]School of Biological Sciences, Chungbuk National University, 1 Chungdae-Ro, Seowon-Gu, Cheongju 28644, South Korea. E-mail: jyahn@chungbuk.ac.kr, kyh@chungbuk.ac.kr
[b]Department of Bioprocess Engineering, Chonbuk National University, 567 Baekje-daero, Deokjin-Gu Jeonju 54896, South Korea
[c]School of Earth Sciences and Environmental Engineering, Gwangju Institute of Sciences and Technology (GIST), 123 Cheomdan-gwagiro, 500-712, South Korea

†Electronic supplementary information (ESI) available. See DOI: 10.1039/c6nr09408b

being touted as an alternative to antibodies, therapeutics and bioelements for sensors, *etc*.[16–18] Aptamers are experimentally selected from a random pool by the Systematic Evolution of Ligands by EXponential enrichment (SELEX) procedure, which is a powerful tool for screening large libraries of randomized nucleic acids (generally 10^{13}–10^{15} different structures). Aptamers can bind to their targets with high affinity and in addition can recognize their targets with high specificity, which is a measure of the type and strength of binding with which the targets bind at the critical sites. They are comparable to antibodies, with the potential for recognition with a wide range of target molecules, including small molecules such as metal ions.[19] Aptamers also are easily modified to incorporate molecular markers or to favour immobilization,[20,21] can be produced and used under non-physiological conditions, and can be recessively denatured, allowing the optimization of reusable electrical sensing devices.[22] Extensive research on aptamers and their generating process, SELEX, has shown that they have great potential for use in a variety of areas, including *in vitro*/*in vivo* diagnosis, molecular therapy, identification of biomarkers, ligand probing for the delivery, bio-imaging and sensing.[17,23,24]

The aptamers occupy a binding site region termed an aptamotif. Recent studies have reported aptamer secondary structures predicted by the M*fold* server for understanding the relationship between specificity and the structure.[25,26] In addition, several other computational methods such as MEMERIS, RNAcontext, RNAprofile, RNAForester, ExpaRNA and LocARNA (or LocARNATE, extended version of LocRNA) are used for identifying potential binding regions and understanding secondary structure information by inputting sequence data sets. However, these approaches are not fully compatible with the requirements for identifying aptamotifs.[27] To gain a better understanding of how copper binds to an aptamotif, the binding site has been suggested based on the secondary structure and the binding affinity of aptamer candidates with copper. The proposed functional site was then mutated and deleted in all aptamers and the change in the binding affinity of copper with mutation and deletion was helpful in understanding the possible copper–aptamotif interactions.

We finally introduce an Aptamer Integrated Recovery Platform (AIRP) for the specific recovery of copper. This system employs a biotinylated specific aptamer (Cu-A2) and streptavidin agarose resin as a solid support. The immobilized aptamer showed high copper recovery efficiency from the laboratory-prepared aqueous copper solution as well as from the mine drainage samples collected from the Dalseong mine in Korea. Moreover, the continuous copper retrieval capability was evaluated from a regeneration experiment repeated over 20 times. Our new approach based on AIRP can lead to the development of a highly reusable and reproducible copper retrieval, separation and enrichment process. Moreover, the characterization of the sequence regions that give rise to copper aptamer binding interactions will also open doors for the modulation and design of more efficient and specific aptamers against copper-reuse with high selectivity and affinity.

Experimental section

Systematic evolution of ligands by exponential enrichment (SELEX) for selection of copper binding aptamers

The aptamers with target specificity and high affinity were experimentally generated using an *in vitro* selection and amplification technology known as SELEX from a random DNA library designed and prepared by Bioneer, Korea (chemical synthesis, purified by PAGE): 5′-GGT AAT ACG ACT CAC TAT AGG GAG ATA CCA GCT TAT TCA ATT-N40-AGA TAG TAA GTG CAA TCT-3′. Asymmetric PCR was used to preferentially amplify one strand of the original DNA more than the other. The asymmetric PCR products were then separated and purified using streptavidin for single-stranded DNA (ssDNA) preparation. The concentration of ssDNA was determined using a Nanodrop spectrophotometer (Thermo Scientific, Wilmington, DE). A copper-chelate affinity column was utilized by immobilizing iminodiacetic acid on an epoxy-activated Separose 6B resin (GE Healthcare, Sweden) according to the manufacturer's instructions. The affinity column (without copper) was applied for the negative selection step.

The aptamer pool from SELEX round 8 was subsequently amplified by PCR using the unmodified primers and cloned into the vector pDrive cloning vector system (Qiagen, USA). Sequence analysis and alignments were performed using Vector NTI (Invitrogen, UK).

DNA template library and primers for PCR amplification

The random DNA library of 100 nt contained two (42 nt and 18 nt) constant regions complementary to the primers at its ends and a 40 nt random region in the middle. The following primers, that anneal the 5′- and 3′-ends of the library, were used to amplify the selected oligonucleotides during the copper aptamer selection process: 5′-GGT AAT ACG ACT CAC TAT AGG GAG ATA CCA GCT TAT TCA ATT-3′ (forward) and 5′-AGA TAG TAA GTG CAA TCT-3′ (reverse). The reverse primer was labelled with biotin at the 5′-end. The random DNA library and PCR primers were custom-synthesized by Bioneer (Daejeon, Republic of Korea). The initial DNA library was generated by PCR using a thermocycler (Mycycler™, Bio-Rad). PCR was carried out in a total volume of 50 μL using the following reagents: 20 mM Tris-HCl, pH 8.3, 50 mM KCl, 2 mM $MgSO_4$, 10 mM $(NH_4)_2SO_4$, 0.1% Triton X-100, 0.2 mM dNTPs, 20 pmol of each primer, and Taq DNA polymerase (Takara, Japan). The random DNA library was added in amounts of 100 ng per reagent mixture. PCR cycling which consisted of the following conditions was repeated five times: 94 °C (30 sec or 5 min), 52 °C (1 min), and 72 °C (1 min). The PCR products were purified using a QIAquick PCR purification kit (Qiagen, USA).

Asymmetric PCR and preparation of single-stranded DNA (ssDNA) aptamers

The 1/10 volume of the purified DNA products served as a template for an asymmetric PCR. The asymmetric PCR reaction was carried out in a 100 μL mixture containing 20 mM

Tris-HCl, pH 8.3, 50 mM KCl, 2 mM $MgSO_4$, 10 mM $(NH_4)_2SO_4$, 0.1% Triton X-100, 0.2 mM dNTPs, 100 pmol of the forward primer, 10 pmol of the biotinylated reverse primer and Taq DNA polymerase (Takara, Japan). Amplification with a thermocycler (Mycycler™, Bio-Rad, USA) consisted of one cycle at 94 °C for 5 min, followed by 15 cycles at 94 °C for 1 min, 52 °C for 1 min and 72 °C for 1 min. The asymmetric PCR reaction was terminated with a final extension step of 7 min at 72 °C. The asymmetric PCR products of 100 μL were precipitated with ethanol at −20 °C to remove the unincorporated primers as well as to reduce the volume. The precipitate was then dissolved in a TE buffer (10 mM Tris-HCl [pH 7.5], 1 mM EDTA), and the final volume of the solution was adjusted to 100 μL. The amplicons were detected by electrophoresis of 2 μL aliquots through 2% agarose gel in 0.5 × TAE (20 mM Tris-acetate [pH 8.5], 1 mM EDTA).

Separation and purification of non-biotinylated ssDNA were carried out using streptavidin. The asymmetric PCR products were added to 100 μL of streptavidin and incubated at 25 °C for 1 h. At the end of the streptavidin reaction, the samples were centrifuged at 13 000 rpm for 20 min. The supernatant was then extracted with phenol/chloroform and precipitated with ethanol. The pellet was resuspended in a 100 μL copper aptamer SELEX buffer (20 mM Na_2HPO_4, 150 mM NaCl, 1 mM imidazole) and the ssDNA product was detected by electrophoresis of 2 μL aliquots through 2% agarose gel in 0.5 × TAE. S1 nuclease was added to 2 μL of the resuspended ssDNA product to a final reaction volume of 10 μL. The resulting mixture was then incubated for 1 h at 37 °C, after which the removal of ssDNA was also confirmed by 2% agarose gel in 0.5 × TAE electrophoresis.

The aptamer pool from the SELEX 8th round that eluted the maximum amount of copper-binding ssDNA was subsequently amplified by PCR using the unmodified primers, and cloned into the vector pDrive cloning vector system (Qiagen, USA). Ligation of the amplified PCR fragments and the pDrive cloning vector was performed overnight at 4 °C using DNA ligase. The ligated product was then transformed into *Escherichia coli* DH5α, in which a 100 μL aliquot was spread over LB agar plates containing ampicillin (60 μg mL^{-1}), IPTG (0.2 mM), X-Gal (40 μg mL^{-1}). This procedure was followed by an overnight incubation at 37 °C. The 40 white colonies were arbitrarily selected and sequenced by using Solgent (Daejeon, Korea) using the appropriate primers (M13F, M13R).

Preparation of copper-immobilized affinity columns for the selection of the copper-binding aptamer

The epoxy-activated Sepharose 6B resin (Sigma-Aldrich) was first activated with distilled water at 25 °C for 5 min, and then incubated with 500 mM iminodiacetic acid at 37 °C for 16 h. The copper affinity column was washed three times with alternatively high and low pH buffer solutions (acetate buffer [0.1 M, pH 4] and Tris-HCl [0.1 M, pH 8], respectively) and then exposed to copper solution (100 mM $CuSO_4$ in Milli-Q water). Prior to incubation with the copper affinity column, the ssDNA pool was denatured at 85 °C for 5 min, allowed to renature at room temperature for 2 h, and the final solution volume was adjusted to 1 mL. The ssDNA aptamer pool of 5 μg was then applied to the column and incubated at 25 °C for 1 h. The ssDNA aptamer bound column was washed twice with five column volumes of 0.1% Tween 20 in the copper aptamer SELEX buffer to remove the unincorporated (non-copper specific) ssDNA aptamer.

To elute the copper binding ssDNA aptamer, the column was incubated with the DNA aptamer elution buffer (20 mM Na_2HPO_4, 40 mM imidazole, 150 mM NaCl) at 85 °C for 5 min. The eluted copper binding ssDNA aptamer was extracted with phenol/chloroform, precipitated with ethanol and then resuspended in 50 μL distilled water.

Identification of the copper aptamer with binding affinity

The interactions between the aptamers (CuA-1, CuA-2, CuA-3 and CuA-4) from the isolated 8th round aptamer pool and the copper immobilized on the affinity column were examined by adding 5 μg mL^{-1} of the Cy5 labeled aptamer on the copper-chelate affinity column and the epoxy-activated Sepharose resin column itself, without copper. All the Cy5-labeled aptamers were synthesized by Bioneer (Korea). The addition of the Cy5 labeled aptamer was followed by 1 h incubation at 25 °C. To elute the ssDNA aptamer, a DNA aptamer elution buffer was added to each column and incubated for 5 min at 85 °C. The eluted ssDNA aptamer was extracted with phenol/chloroform and precipitated with ethanol, in which its pellet was resuspended in 50 μL distilled water and then spotted onto the amino coated slides (UltraGAPS Coated Slides, Corning). The fluorescence intensity of the spotted ssDNA aptamer was measured using a GenePix 4000B, Axon laser scanner. The concentrations of the eluted ssDNA aptamer were determined using a Nanodrop spectrophotometer (Thermo Scientific, Wilmington, DE).

Assessment of binding affinity and specificity using surface plasmon resonance (SPR)

The binding affinities of the 4 selected aptamers (Cu-A1 to Cu-A4) from the 8th round were analyzed by surface plasmon resonance (SPR) at 25 °C using a Biacore 3000 instrument (Biacore AB, Sweden). For conjugating copper, a nitrilotriacetic acid (NTA) immobilized sensor chip (sensor chip NTA, Biacore) was exposed to copper solution (100 mM $CuSO_4$ in Milli-Q water) for 4 min at a flow rate of 5 μL min^{-1}. For control experiments the sensor surface was treated as above, but EDTA (1 μM) was injected for 4 min. After the baseline stabilization, the four ssDNA aptamers (Cu-A1 to Cu-A4) selected from round 8 were sequentially injected onto the sensor surface to measure the binding affinity (K_D) of the copper–aptamer interactions as recommended by the manufacturer's manual. After each measurement, the sensor chip was regenerated by stripping Cu(II) from the surface and cleaning the flow system Cu(I) with 100 μL of 1 mM bicinchoninic acid (BC, copper chelator), 50 mM HEPES/NaOH, pH 7.2, 50 mM KCl, 5 mM $MgCl_2$ and 50 mM EDTA (injected at a flow rate of 5 μL min^{-1}). The

binding affinity (K_D) value of the isolated aptamers was calculated using the BIA evaluation software, version 4.1.

To determine the specificity of the aptamer, the streptavidin coated sensor chip SA was used which was initially equilibrated with HEPES and activated with 50 mM NaOH, 1 M NaCl at 5 μL min^{-1} for 10 min.[28] 100 μM of the biotinylated aptamer (Cu-A2) with the highest affinity to copper was then injected into the sensor chip. All metal samples were dissolved or diluted in Milli-Q water. Each of the following heavy metal resulting solutions: 0.1 M $MgCl_2$, 0.1 M $NaAsO_2$, 0.1 M $NiCl_2$, 0.1 M $CoSO_4$, 0.1 M $CaCl_2$, 0.1 M $FeCl_2$, 0.1 M $MnCl_2$, 0.1 M $CdCl_2$, and 0.1 M $ZnCl_2$ was individually introduced into the aptamer bound SA sensor chip, and the K_D of the aptamer was measured. After each experiment, the sensor chip was regenerated with 0.5% SDS. The background response was also recorded by injecting the metal samples through a reference flow cell, which has no aptamer immobilized on the sensor surface. The background response was then subtracted from the sensorgram to obtain the actual binding response. The BIA evaluation program, version 4.1, was used to analyze the binding kinetics of the copper binding aptamer and various other heavy metals.

Mutation and deletion of the predicted aptamotif region

To confirm the binding of copper at the predicted aptamotif site, the nucleotides at the predicted binding site were mutated and deleted. The same experimental conditions as used for the native aptamer were applied to determine the binding of copper with mutated and deleted aptamers by SPR analysis. Secondary structures of the mutated and deleted aptamers were depicted using the Zuker algorithm, M*fold.*[29]

Copper recovery from aqueous solutions

In order to investigate the recovery of copper by the selected aptamer, streptavidin agarose resin was used. The aptamer conjugation procedure was composed of the following: (1) a total 200 μL of streptavidin agarose resin (Thermo Scientific, USA) was added to 1.5 mL of a microtube. (2) After centrifuging it for 1 min, the supernatant was removed and the resin was washed twice with 1 ml of the SELEX buffer. (3) 2 mg of the biotinylated aptamer was dissolved in 400 μL of the SELEX buffer and applied drop-by-drop on to the streptavidin agarose resin and was incubated for 1 h on a thermomixer (Eppendorf, Germany) at 1300 rpm. After this incubation step, streptavidin agarose resin was prepared without the aptamer as a negative control. (4) Prior to introducing copper solutions, non-bound aptamers were removed by extracting the supernatant and the resins were thoroughly rinsed with SELEX buffer. (5) After washing, 1 mL of copper solutions was transferred to both streptavidin-agarose resins with and without the aptamer and incubated for 2 h at 25 °C in a 1.5 mL reaction tube (final concentrations, 1, 3, 5, 7, 10, 30, 50, 70, 100, 150 and 300 mg L^{-1}). (6) After centrifugation at 13 000 rpm for 1 min, the copper content in the supernatant fraction was measured by Inductively Coupled Plasma-Mass Spectrometry (ICP-MS, Agilent 7500ce, Agilent, USA). Subsequently, the copper recovery on the solid resins was obtained by SEM imaging. The entire process of binding and copper measurement was repeated, and all experiments were performed in triplicate.

The morphology of the copper bound streptavidin-agarose resins was obtained by using a field emission scanning electron microscope (FE-SEM, LEO 1530, LEO, Oberkochen, Germany). For imaging, three types of samples were prepared as the following; (a) streptavidin agarose resin, (b) aptamer conjugated streptavidin agarose resin, and (c) copper–aptamer conjugated streptavidin-agarose resin.

Copper recovery from the mine drainage of the local sites

Immediately after the copper recovery test with laboratory prepared copper solutions, the copper specific aptamer, Cu-A4, was applied to the mine drainage samples collected from the Dalseong (DS) copper–tungsten mine in Daegu city, South Korea: DS-1 (35°77′75″N, 128°66′99″E), DS-2 (35°77′74″N, 128°66′86″E), and DS-3 (35°77′74″N, 128°66′84″E). These mine drainage samples were analyzed according to the method reported in the literature.[30] The recovery procedure is identical to the method used to recover copper from the laboratory prepared aqueous solutions as described above. 1 mL of each mine drainage solution was introduced into the aptamer conjugated streptavidin-agarose resin. After incubation for 5 min at 25 °C on a thermomixer (Eppendorf, Germany) at 1300 rpm, all tubes were centrifuged for 1 min. And then the copper and other constituents present in three mine-drainage samples were measured from the supernatant solutions using ICP-MS.

Reusability determination of the Cu-A2 aptamer conjugated streptavidin resin

The reusability of the copper-specific aptamer conjugated streptavidin-agarose resin and copper retrieval were examined. Briefly, the aptamer regeneration comprised of 4 steps, including copper binding to the aptamer–resin complex (step 1), heat-denaturation of the aptamer and copper retrieval (step 2), renaturation of the aptamer on the resin (step 3) and reincubation of the copper solution (step 4). The aptamer–resin complex and copper solution were repetitively used during the entire regeneration cycles. The initially prepared copper concentration was 20 mg L^{-1}, which was measured by ICT-MS before its use.

Prior to regeneration experiments, the specific aptamer, Cu-A2 was biotinylated and incorporated into the streptavidin agarose resin. The Cu-A2 conjugated streptavidin agarose resin complex was equilibrated by washing two times with a SELEX buffer solution. The complexes were incubated with the initial copper solution (20 mg L^{-1}) at room temperature for over 2 h and then centrifuged at 13 000 rpm for 1 min, to remove unbound copper. The copper bound complexes were dissolved with 1 mL of SELEX buffer and heat-treated for 15 min at 85 °C, to release copper from the aptamers, with vigorous vortexing using a thermomixer (Eppendorf, Germany). Following centrifugation for 5 min at 13 000 rpm, the supernatant, which contains the copper, was collected for the next cycle and the concentration was measured by ICT-MS for determining the

copper retrieval. Subsequently, the Cu-A2 on the streptavidin agarose resin was carefully denatured by heating for 15 min at 85 °C in SELEX buffer and then renatured by incubating for 2 h at 25 °C. The regeneration experiment consists of 20 cycles, in which aptamer–resin complexes were introduced into the supernatant, which was collected from the previous cycle, for the next cycle.

Results and discussion

Selection and identification of copper-binding aptamers

The ssDNA library that contained 40-mer random DNA sequences flanked by two PCR primer sequences has been utilized in the present study. The target, copper, was immobilized on epoxy-activated Sepharose 6B resins, which allows easy and effective handling of the SELEX process (Fig. 1). During the 9th round of the SELEX process, the specifically bound ssDNA aptamers were enriched by excluding a nonspecific and/or a weak binder. After 7 cycles, we specially applied negative selection (NS) along with positive selection, as negative selection sometimes hinders positive selection. To remove non-specific binders, negative selection was performed using the bare epoxy resin (without copper) after the 7th round and a total of 10 rounds of selection were carried out.

The overall SELEX progress was monitored by comparing the concentration of all eluents as shown in Fig. 2. We calculated the amount of DNA eluents from the entire 9 round selections. The enrichment of the selected ssDNA pools was proportional to the increase in round number. At the 8th round of selection, the concentration of the enriched ssDNA pool was observed to be substantially higher. Thus, the 8th round ssDNA was used in the cloning procedure and 40 clones were sequenced to identify individual aptamer candidates. The 11 aptamers with binding affinity values ranging from 10^{-11} to 10^{-8} K_D (M) were listed and 4 high affinity aptamers were finally selected from among 11 candidates. All sequence data and affinity have been included in ESI Table S1.†

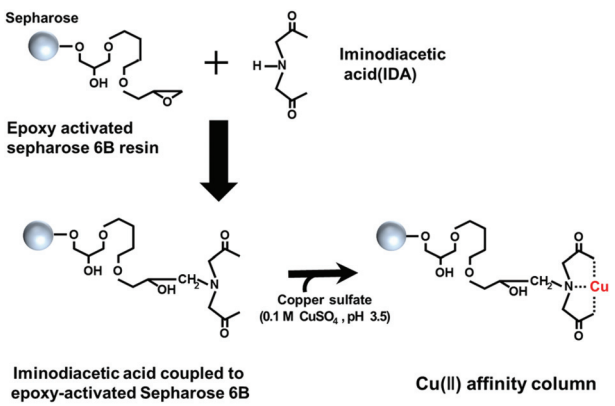

Fig. 1 Coupling reaction of copper on an epoxy activated Sepharose 6B resin. A copper-chelate affinity column was utilized by immobilizing iminodiacetic acid on an epoxy-activated Separose 6B resin.

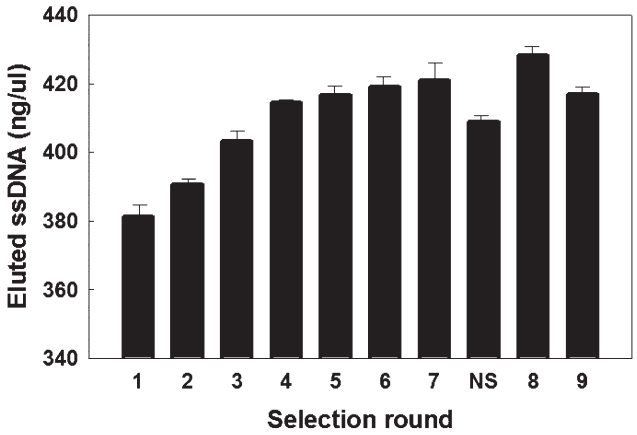

Fig. 2 Concentrations of the eluted copper-binding ssDNA from SELEX selection rounds (NS: negative selection). The aptamer pool from SELEX round 8 that eluted the largest amount of copper-binding ssDNA was subsequently amplified by PCR using the unmodified primers, and cloned into the vector pDrive cloning vector system (Qiagen, USA). Asymmetric PCR was used to preferentially amplify one strand of the original DNA more than the other. The asymmetric PCR products were then separated and purified using streptavidin for single-stranded DNA (ssDNA) preparation.

The binding affinity of the selected aptamers was investigated by using surface plasmon resonance (SPR)-based Biacore 3000 instrument. Using 100 mM $CuSO_4$ solution, copper was coupled on the substrate of the NTA sensor chip by chelate chemistry. After immobilizing copper, each aptamer was applied to the NTA sensor chip. The K_D value of the isolated aptamers was calculated using the BIA evaluation software, version 4.1. The K_D values of the copper-binding aptamers are in the picomolar range and lie between 1.83×10^{-11} M and 8.95×10^{-10} M. From the SPR data of 4 aptamers, it has been observed that Cu-A2 can bind to copper with a K_D value of 1.83×10^{-11} M, which shows the highest affinity to copper (see ESI Fig. S2 and Table S2†). Cu-A1 has binding affinity similar to that of the Cu-A2 aptamer, whereas that of Cu-A3 and Cu-A4 is 10-fold lower (Cu-A1, 7.88×10^{-11} M; Cu-A2, 1.83×10^{-11} M; Cu-A3, 8.95×10^{-10} M; Cu-A4, 1.73×10^{-10} M).

In vitro binding assays were conducted for the 4 aptamers (Cu-A1 to Cu-A4) selected to evaluate their binding affinities between the aptamer and copper (Fig. 3). All aptamer candidates and the random ssDNA library (control) were labelled with Cy5 and applied to two types of resins, namely the copper-chelate epoxy resin and the bare epoxy resin. After incubating and washing, the aptamers were eluted from the copper chelate resin and bare epoxy resin in parallel. The concentration of the eluents was calculated and simultaneously spotted onto the surface of amino-coated slides. The DNA concentrations and fluorescent activity were compared with each other. Out of the 4 aptamer candidates examined in the present study, Cu-A2 binds to copper with high binding properties. Even though we confirmed that the isolated aptamers did not react with the solid support, affinity resin, aptamer Cu-A3 showed negligible fluorescent binding activity to

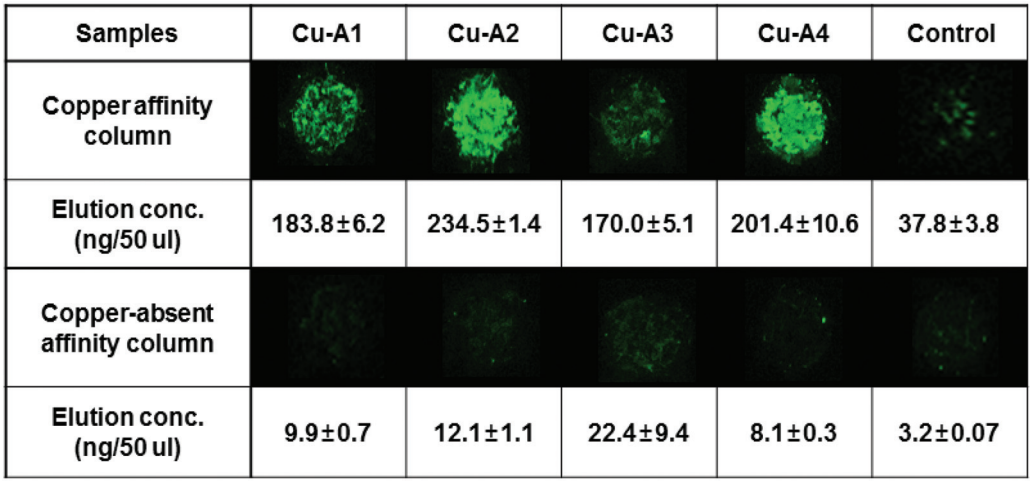

Fig. 3 The interactions between the 4 aptamers and the copper immobilized on the affinity column were examined by adding 5 μg of the Cy5 labeled aptamer to the copper-chelate affinity column and to the epoxy-Sepharose resin column, without copper. The fluorescence intensity of the spotted ssDNA aptamer was measured using a GenePix 4000B, Axon laser scanner. The concentrations of the eluted ssDNA were determined using a Nanodrop spectrophotometer (Thermo Scientific, Wilmington, DE). Control: random ssDNA library.

copper. The copper binding aptamers we isolated have their K_D values ranging from pico to nanomolar affinity. These results for aptamer binding affinity show good agreement with our previous research paper.[31] The high affinity may be due to the following reasons: (1) the efficient separation of the target binder in the discrimination step, (2) an appropriate binding environment (buffer, temperature, time, *etc.*) and (3) the target properties *etc.*

Defining the potential copper binding motif by a mutation and deletion analysis

We analysed the importance of the secondary structure of the copper-binding aptamer by varying G–C stem components and measuring the copper binding affinity of these constructs. The secondary structures of the Cu-A2 were depicted using the Zuker algorithm, M*fold*,[29] and are given in Fig. 4. Several studies have reported aptamer secondary structures predicted by the M*fold* server for understanding the relationship between specificity and the structure.[25,26] The preference of copper binding to G–C pairs rather than A–T pairs has already been reported in studies on copper binding schemes.[32–36] The potential copper binding site has been predicted on the basis of the sequence, secondary structure, and the binding affinity (K_D) of aptamer candidates with copper. The predicted secondary structure of Cu-A2 shows the combinations of two stems of 5 G–C and a continuous single stranded bridge, which could be a potential copper binding region, aptamotif. Based on these observations and previous reports, we assumed that the highest binding affinity of Cu-A2 relies on the 5 G–C pairs of the secondary structures, G20/C45, G21/C44, G22/C43, G48/C58, and C49/G57 at positions 1–8 nt (Fig. 4, Cu-A2nat, the number of 1–8 nt corresponds to 43–50 nt). In order to validate our prediction, the nucleotides at position 1 to 8 nt were mutated (A/T → G/C, G/C → A/T) (Fig. 4, Cu-A2mut). The binding affinity of copper with the mutated aptamers was calculated and compared with the native aptamers. The changes in the binding affinity of copper with the mutated aptamer provide insights into the potential binding interaction of copper with these aptamers.

It was observed that the single stranded bridge is critical to maintain high copper binding affinity. With the mutation of G, C nucleotides with A, T at the binding motif, the binding affinity has reduced by 100-fold. Even the formation of 5 G–C pairs and 1 A–T pair in the mutated aptamer (position 50 to 58) has not affected the copper binding affinity as in the case of the native aptamers. This result implies that the presence of 5 G–C pairs in the mutated Cu-A2 aptamer does not cause any significant change in the binding affinity even though the number of G–C pairs is still high, confirming the binding of the aptamer at location 1–8 nt. The low binding affinity even in the presence of 5 G–C pairs in the mutated Cu-A2 aptamers can be attributed to the presence of the A–T–A single stranded bridge between the two stems as compared to the presence of the A–G sequence for the native Cu-A2 aptamer.

From the mutation and deletion analysis, we have confirmed that the high G–C pairs and stem-interval distance play important roles in copper binding. Our analysis revealed that the secondary structure significantly contributes to the stability and physical affinity of the aptamers. In order to validate the full potential of the Cu-A2 aptamotif for copper binding, the aptamotif region (1 to 8 nt) was eliminated (Fig. 4, Cu-A2del). The deleted Cu-A2 has 4 G–C and 1 A–T which shows a similar binding configuration with native Cu-A2, however its binding affinity was 1000-fold lower than the native aptamer. Overall, only a small fraction of sequences, "(5′)-CCCAGGCT-(3′)", in Cu-A2 formed an energetically favour-

Aptamer		Sequence (N_{40})	K_D (M)
Cu-A2	Nat	CCCAGGCTTGGATAGCACATTCATGGCAGCGTTCTTTACG	1.83×10^{-11}
	Mut	ATAGATACTGGATAGCACATTCATGGCAGCGTTCTTTACG	8.34×10^{-9}
	Del	TGGATAGCACATTCATGGCAGCGTTCTTTACG	4.84×10^{-8}

Aptamer		Sequence (N_{40})	K_D (M)
Cu-A1	Nat	GGTGTGACTGAGTAACTCACTCCAACCCCTGGAGTGGGAT	7.88×10^{-11}
	Mut	AACTGAGTTGAGTAACTCACTCCAACCCCTGGAGTGGGAT	7.65×10^{-10}
	Del	TGAGTAACTCACTCCAACCCCTGGAGTGGGAT	3.97×10^{-9}

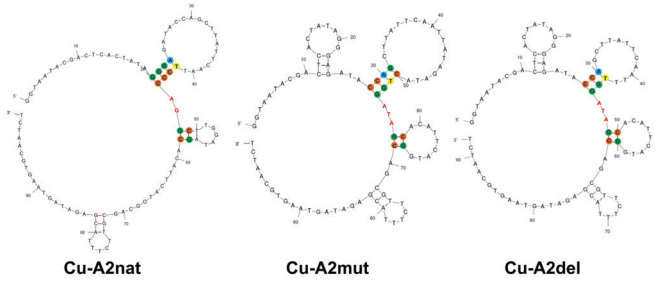

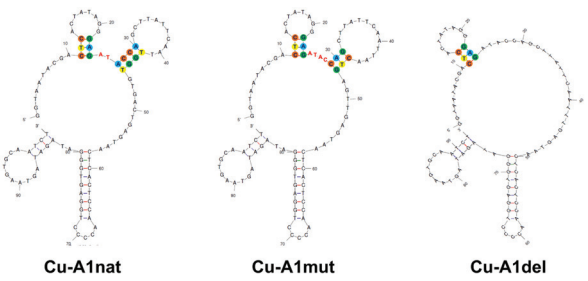

Aptamer		Sequence (N_{40})	K_D (M)
Cu-A3	Nat	ATTTGACCATCGTCTCCGGCTCACGGAATTATCAGCAGCG	8.95×10^{-10}
	Mut	GGGGTGTTATCGTCTCCGGCTCACGGAATTATCAGCAGCG	8.50×10^{-11}
	Del	ATCGTCTCCGGCTCACGGAATTATCAGCAGCG	1.69×10^{-8}

Aptamer		Sequence (N_{40})	K_D (M)
Cu-A4	Nat	TTCTTAGGGAAGTAATCACGGAAAACCGTCTCCGTTCTCA	1.73×10^{-10}
	Mut	CCAGGCAAGAAGTAATCACGGAAAACCGTCTCCGTTCTCA	7.73×10^{-11}
	Del	GAAGTAATCACGGAAAACCGTCTCCGTTCTCA	1.92×10^{-10}

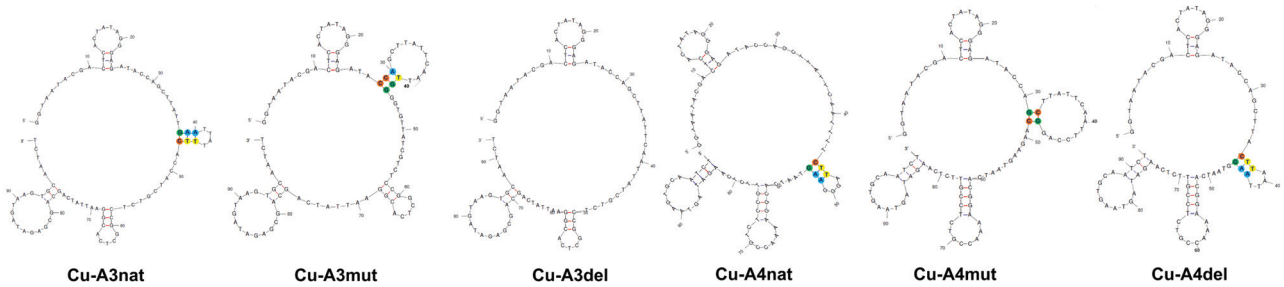

Fig. 4 The secondary structure of aptamers and binding affinity analysis. The secondary structures of Cu-A1 to Cu-A4 with mutation and deletion were predicted at 25 °C with 150 mM NaCl using the Zuker's algorithm, M*fold*. Potential binding sites are highlighted with colour dots and red-bold characters in native, mutated, and deleted aptamers. The SPR data are listed in ESI Table S3.†

able active secondary structure, 5 G–C pairs and an A–G bridge, hence indicating a high binding mechanism between the Cu-A2 and copper.

The importance of the stem-interval distance was clearly observed in Cu-A1. The aptamer Cu-A1 is the second best binding affinity aptamer with a K_D value of 7.88×10^{-11} M and shows the combinations consisting of two stems of 4 G–C pairs (C11/G24, C13/G22, C28/G44, and C29/G43) and a sandwiched single stranded A–T bridge between position 25 and 26 in a random (N_{40}) sequence region (Fig. 4, Cu-A1nat). The extended long-length bridge configuration (4 nt single strands between position 25 and 28) might be the cause of the weakened binding affinity (Fig. 4, Cu-A1mut), showing that the Cu-A1mut binds with a 10-fold lower affinity than Cu-A1nat. The deletion of the G–C stem region from the aptamer, Cu-A1del, has a binding affinity of 3.97×10^{-9} M, which is probably due to the absence of G–C pairs in the deleted region, "(5′)-GGTGTGAC-(3′)", (Fig. 4, Cu-A1del).

We analysed the importance of the increase of G–C pairs in copper binding affinity using Cu-A3 and Cu-A4. The native Cu-A3 aptamer interacts with copper with a binding affinity of 8.95×10^{-10} M and 1 G–C and 2 A–T pairs are present at the random sequence region (Fig. 4, Cu-A3nat). The mutation of the G–C pair (G38/C47) at the site, (5′)-ATTTGACC-(3′), results in a 10-fold increase in the binding affinity to 8.50×10^{-11} M, which is probably due to an increase in the number of G–C pairs at the binding site to 2 G–C pairs (Fig. 4, Cu-A3mut). However, the deletion of the G–C pairing region from the aptamer results in a structural change, resulting in a K_D value of 1.69×10^{-8} M (Fig. 4, Cu-A3del). On comparing the Cu-A4nat and Cu-A4del, the mutated Cu-A4 aptamer has 2 G–C pairs at the random site. The binding affinity for Cu-A4nat is 1.73×10^{-10} M and 7.73×10^{-11} M for Cu-A4mut and 1.92×10^{-10} M for Cu-A4nat. The presence of 2 G–C pairs (C31/G46 and C32/G47) at (5′)-CCAGGCAA-(3′) for Cu-A4mut likely influences strong binding of copper to the aptamer. The above results observed after mutation and deletion clearly indicate that the stem-interval distance and the increase of the G–C pair might play an important role in the structure stability of the binding site and high binding affinity to copper. Actually, the mutation and deletion study is not critical to show the metal-binding motif in the aptamer. Furthermore, the aptamer–metal crystal study will demonstrate some of the biochemical evidence as a direct strategy.

Aptamer specificity analysis for copper

To further demonstrate the binding specificity of the Cu-A2 aptamer, a binding experiment was continuously performed against various other metal ions. Since nine metals ($MgCl_2$, $NaAsO_2$, $NiCl_2$, $CoSO_4$, $CaCl_2$, $FeCl_2$, $MnCl_2$, $CdCl_2$, and $ZnCl_2$) are often found naturally in the environment, so these were chosen as a test panel. First of all the biotinylated aptamer, Cu-A2, was loaded onto the streptavidin coated sensor chip-SA (StreptAvidin). The metal solutions were then separately passed through the surface immobilized with the aptamer. As shown in Fig. 5, the Cu-A2 aptamer showed the lowest K_D values to copper. Even if there are similar structures close to the binding region of the target (sulfate group of $CoSO_4$), Cu-A2 was able to better recognize copper (see the results of $CuSO_4$ and $CoSO_4$).

The above results indicated that Cu-A2 could bind indeed specifically to copper. In order to determine if this binding activity would be retained when the aptamer was immobilized on the 3-dimensional solid phase, the streptavidin agarose resins covered with biotinylated Cu-A2 were incubated with copper solutions (100 mg L^{-1}) for 60 min. Aptamer conjugation steps are provided in ESI Fig. S1.† The entire resins were concentrated under mild conditions (13 000 rpm, 1 min). The supernatant was discarded and the pellet was washed with SELEX buffer solution. The morphology of the functionalized aptamer-streptavidin agarose resin was studied by FE–SEM. SEM images presented in Fig. 6 show the appearance of the bare streptavidin agarose resin (a), Cu-A2 conjugated resin (b) and copper binding on the surface of the Cu-A2 conjugated resin (c). The streptavidin agarose resins have a spherical form and smooth surface which may be formed during the polymerization and protein (streptavidin) coating processes. The biotinylated Cu-A2 could be fully bound on the surface of the resin with the 3-dimensional solid phase, providing a large surface area for the binding target, copper. In comparison to the streptavidin agarose resins, Fig. 6(a), the morphological feature of Fig. 6(b) shows a slight change to be rough, probably due to the binding of aptamer species on the surface. After achieving the copper, the surface of Cu-A2 bound resins was covered thick with scraps of copper as shown in Fig. 6(c). It should be noted that the presence of Cu-A2 affects the copper binding on the solid phase and might be applicable to the large scale pull-down approaches.

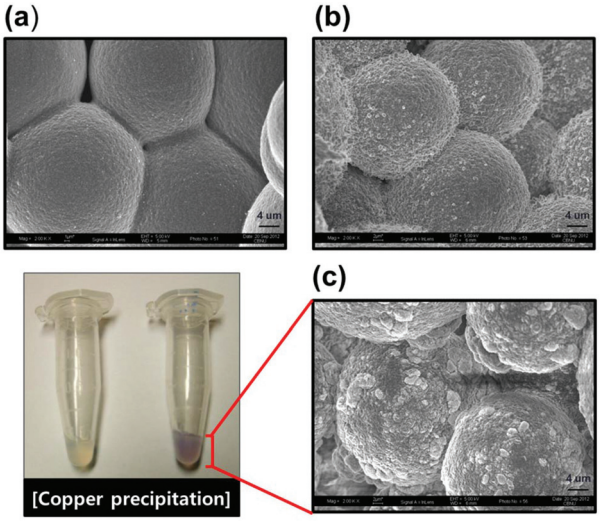

Fig. 6 Field emission scanning electron micrographs (FE-SEM) of the (a) control, streptavidin agarose resins, (b) biotinylated aptamer immobilized streptavidin agarose resins, and (c) copper bound-biotinylated aptamer conjugated streptavidin resins. Copper recovery by colorimetric detection was accessed by using the biotinylated aptamer conjugated streptavidin agarose resins, (left, whitish colour) before and (right, bright purple) after addition of 100 μL of 0.1 N NaOH solution.

Furthermore, it was sufficiently effective to visualize copper recovery. Copper binding and capture by using Cu-A2 conjugated resins was observed by Cu precipitation reaction methods.[37] The evidence that this reaction occurred was the visible change in color to purple, in addition to the formation of a precipitate. In detail, when sodium hydroxide (0.1 N) was treated with the copper bound aptamer resin, copper was precipitated by copper chemistry and turned purple (Fig. 6, see copper precipitation). The change of color and density of the precipitate may further give an indication of the amount of copper.

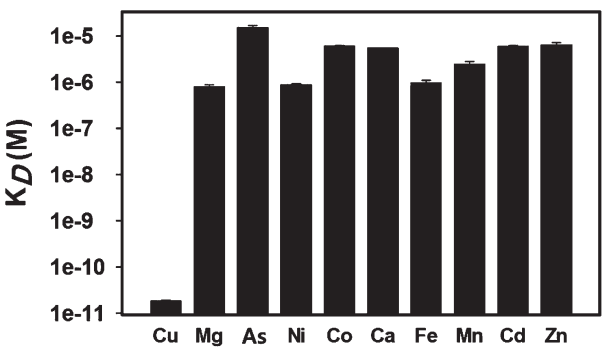

Fig. 5 K_D values of Cu-A2 to copper and nine different metals determined individually.

Copper recovery from aqueous solutions using the copper-binding aptamer Cu-A2

Having observed that Cu-A2 showed copper binding activity, even when immobilized on a solid substrate, the next goal of this study was to determine if Cu-A2 could be used to recover copper from different aqueous samples. It is well known that copper is one of the essential materials in natural resources. The selective separation, enrichment or recovery of valuable metals would lead to an improved exploitation of the available potential in industry. We here designed an Aptamer Integrated Recovery Platform (AIRP) for recovering copper. AIRP basically employed streptavidin agarose resin as a solid support and a biotinylated specific aptamer, *i.e.* Cu-A2. In fact, streptavidin,

Table 1 AIRP-copper recovery activity in aqueous solutions

Copper conc. (mg L^{-1})	Copper determined (mg L^{-1})		
	Initial copper conc.[a]	Streptavidin agarose resin[b]	AIRP (aptamer conjugated)
1	0.98 ± 0.03	**0.98 ± 0.07**	**N.D.**
3	2.86 ± 0.06	**2.73 ± 0.03**	**N.D.**
5	5.02 ± 0.08	**4.92 ± 0.07**	**N.D.**
7	6.90 ± 0.02	**6.94 ± 0.10**	**N.D.**
10	9.92 ± 0.14	**9.20 ± 0.12**	**N.D.**
30	29.42 ± 0.23	**27.7 ± 0.18**	**N.D.**
50	47.31 ± 0.78	**48.25 ± 0.29**	**N.D.**
70	69.04 ± 0.60	**67.57 ± 0.58**	**0.47 ± 0.25**
100	97.69 ± 1.05	**92.88 ± 0.77**	**0.90 ± 0.56**
150	147.74 ± 1.72	145.63 ± 1.20	38.91 ± 1.08
300	287.11 ± 2.34	282.07 ± 1.58	192.5 ± 1.77

[a] Initial copper concentrations were measured by inductively coupled plasma mass spectrometry (ICP-MS) before it use. [b] Streptavidin agarose resin was used as a negative control as described in the Experimental section. ND stands for not determined.

which is capable of binding up to four biotin molecules, has been well studied and it has very high affinity for biotin conjugated biomolecules. Due to these significant properties, streptavidin is commonly used together with several solid substrates such as resins, beads, and glass slides for specific detection of biotinylated molecules. Since the specific affinity of Cu-A2 was confirmed, so we expected that the AIRP can specifically capture and recover copper from the aqueous solutions.

The effect of AIRP in copper recovery was studied in the presence/absence of Cu-A2 with different copper concentrations as described in Table 1. Aptamer conjugation steps are provided in ESI Fig. S1.† After incubation, the retained copper in the supernatant was measured and compared between an aptamer conjugated AIRP and a non-conjugated negative control. As can be seen from the data, the influence of Cu-A2 in AIRP was clearly observed in the concentration range from 1 to 100 mg L^{-1}, demonstrating successful recovery of copper, approximately over 99%. However, in the aptamer non-conjugated streptavidin, it was observed that the most copper was retained in all the concentration ranges studied. Therefore, the maximum copper binding capacity is 1–100 mg L^{-1} and we further selected the test copper concentration, 20 mg L^{-1}, as the representative concentration for the regeneration activity test.

Copper recovery from mine drainage samples using the copper-binding aptamer Cu-A2

The ability of copper recovery by AIRP was evaluated with the mine drainage samples collected from the local sites in South Korea. Several papers have reported that mine drainage is becoming a serious pollution problem, which is considered as one of the worst environmental problems of mining activities owing to low pH and the presence of high concentrations of heavy metals and other toxic elements.[38,39] The most common treatment methods for mine drainage are chemical methods, *e.g.* the neutralization using lime or other alkaline components. This treatment results in the precipitation of sulphate anions and heavy metal cations in the form of gypsum and metal hydroxides, respectively, which have been discharged. The operating costs of these processes are high, whereas sulphate and metal removal efficiencies are relatively low.[40]

In addition, all the valuable metals are lost in the sludge. Keeping this in mind, we performed AIRP experiments using three local copper-mine drainage samples (DS-1, DS-2, and DS-3) which were collected from the sites in Dalseong (DS), Korea. The initial copper content measured by ICP-MS was 4.532 mg L^{-1} in DS-1, 2.669 mg L^{-1} in DS-2, and 1.283 mg L^{-1} in DS-3. In addition, all mine drainage samples also contain calcium, cadmium, iron, manganese, nickel *etc*. and are acidic with a low pH (3–4). The influence of the aptamer, Cu-A2, on AIRP was investigated and the results are shown in Table 2. As seen, the complete copper recovery was observed in all the three samples, even under acidic conditions, while there was no difference in the content of other metal components after treatment with aptamer-conjugated resins. In fact, the extreme pH should be avoided because it can disrupt the aptamer folding, aptamer–target interaction, and/or target denaturation. Nevertheless, it is important to note that the aptamer binding activity was maintained stably in the local mine drainage samples. This is very important and is of great advantage over other recovery techniques, in which the recovery capacity is reduced by many interfering factors such as the presence of other metal ions and pH.

Reusability of the copper binding aptamer conjugated AIRP and copper retrieval

In order to investigate the reusability of the aptamer and continuous copper recovery based on AIRP, the aptamer–resin complexes were subjected to multiple repeated binding experiments. The recovery efficiency was calculated by measuring the concentration of the applied copper and bound copper, which was calculated by subtracting the amount of free copper in the

Table 2 AIRP-copper recovery activity in mine drainage samples

Metal parameters	DS-1		DS-2		S-3	
	NT[a]	T[b]	NT[a]	T[b]	NT[a]	T[b]
Cu (mg L^{-1})	**4.532**	**N.D.**	**2.669**	**N.D.**	**1.283**	**N.D.**
Cr (mg L^{-1})	0.012	0.005	0.009	N.D.	0.008	N.D.
Ca (mg L^{-1})	340.4	325.8	174.6	165.2	200.7	187.5
Cd (mg L^{-1})	0.159	0.071	0.102	0.053	0.051	0.028
Fe (mg L^{-1})	189.0	187.2	15.90	15.84	1.830	1.821
Mg (mg L^{-1})	115.2	114.7	61.83	61.45	62.48	61.97
K (mg L^{-1})	2.209	2.207	1.906	1.907	3.211	3.198
Na (mg L^{-1})	17.46	17.44	11.39	11.23	14.63	14.64
Ni (mg L^{-1})	0.098	0.094	0.055	0.052	0.039	0.042
Si (mg L^{-1})	29.29	29.20	36.20	36.24	29.38	29.37
Sr (mg L^{-1})	1.089	1.089	0.672	0.673	0.803	0.799
Pb (mg L^{-1})	0.044	0.036	0.014	0.005	N.D.	N.D.
Zn (mg L^{-1})	12.23	11.85	6.038	5.876	3.846	3.449
pH	**4.410**	**4.420**	**3.070**	**3.070**	**3.790**	**3.790**

[a] NT (not treated). [b] T (treated). ND stands for not determined.

supernatant solution from the applied copper. The efficiency of copper recovery was calculated as:

$$E_{\text{Recovery}} = \frac{C_{\text{bou}}}{C_{\text{app}}} \times 100 \quad (1)$$

where C_{app} and C_{bou} are the copper concentrations of the applied test sample and bound copper by the aptamer, Cu-A2, respectively. Retrieval efficiency was calculated by measuring the concentration of copper in the supernatant after heat-denaturing (85 °C for 15 min) of the aptamer. It is defined as:

$$E_{\text{Retrieval}} = \frac{C_{\text{sup}}}{C_{\text{bou}}} \times 100 \quad (2)$$

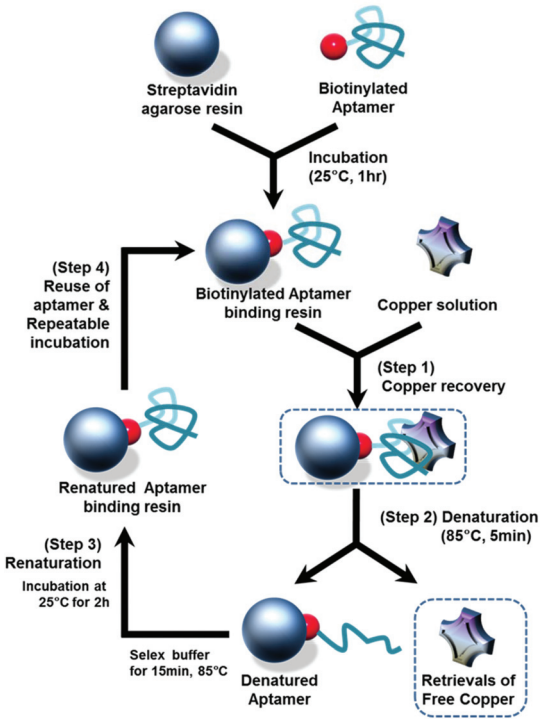

Fig. 7 Schematics of the copper-regeneration process.

where C_{sup} is the concentration of copper in the supernatant, which was released from Cu-A2 after heat treatment.

As we know, unlike other affinity reagents, aptamers can undergo several cycles of denaturation and regeneration so this allows our AIRP to be recyclable, reusable and economic. As illustrated in Fig. 7, the cycled experiments were performed to show the reusability and regeneration capability of AIRP. In all these processes, the interactions between the biotinylated aptamer and streptavidin agarose resin can be stable as per manufacturer's instructions (heating at 85 °C for 15 min), without any deterioration of their interaction properties, which is essential for the repeated use of the copper recovery. After the interaction between the aptamer and resins, the complexes were incubated with the initially prepared copper solution (20 mg L^{-1}), and the recovery efficiency was found to be 100%, which kept capturing in the Cu-A2 conjugated agarose resin. These were then heat-treated to disturb an aptamer tertiary structure and target binding. Bound copper was released to the supernatant fraction and the calculated retrieval efficiency was almost over 99%. The supernatant was then subjected to the next round of the regeneration cycling test. The entire regeneration process was 20 times cycled and data are summarized in Table 3. It is found that the copper has been completely and successfully retrieved during the whole regeneration rounds, even though the slight decrease (89.6% at the 20$^{\text{th}}$ round) in copper recovery has been observed. The decline in the recovery amount might be attributed to the ion absorption[41] inaccurate tertiary structure,[42] non-enzymatic depurination[43] *etc.*, during the repeated heat-processes of denaturation and renaturation. The AIRP proposed by us provided not only the repeatable use of an aptamer, but also the continuous copper recovery in an aqueous environment.

Conclusions

Aptamers can be experimentally identified through the SELEX protocol. The species in the initial pool are enriched, hence having specificity and selectivity depending on their sequence and structure. Copper binding aptamers were identified and their specific binding motifs, aptamotifs, were then predicted

Table 3 Reusability results of copper recovery on AIRP and effective retrieval

Rounds	Copper conc. (C_{app}, mg L^{-1})	Recovered copper (C_{bou}, mg L^{-1})	Recovery efficiency (E_{Recovery}, %)	Released copper (C_{sup}, mg L^{-1})	Retrieval efficiency ($E_{\text{Retrieval}}$, %)
1	**20.03 ± 0.03**[a]	20.02 ± 0.07	100	20.07 ± 0.12	**100**
2	20.07 ± 0.12	20.02 ± 0.19	99.8	20.03 ± 0.19	**100**
3	20.03 ± 0.19	19.99 ± 0.09	99.8	19.96 ± 0.08	**99.8**
5	19.95 ± 0.07	19.93 ± 0.12	99.6	19.88 ± 0.03	**99.7**
7	19.81 ± 0.15	19.79 ± 0.03	98.9	19.75 ± 0.11	**99.8**
10	19.13 ± 0.05	19.14 ± 0.17	95.6	19.15 ± 0.21	**100**
12	19.01 ± 0.18	18.78 ± 0.05	93.9	18.77 ± 0.03	**99.9**
15	18.35 ± 0.09	18.46 ± 0.23	92.3	18.49 ± 0.09	**100**
20	17.99 ± 0.21	17.92 ± 0.13	89.6	17.87 ± 0.07	**99.7**

[a] Initial copper sample concentration was approximately 20 mg L^{-1}.

based on the secondary structure modelling program, the M*fold* program. In fact, it is well known that aptamer species are very functional based on their sequence and structure properties. Although the secondary structures can be manually predicted by the program such as M*fold*, it is still not understandable how aptamers can fit into the cavities of their counterparts, and can have strong dependency on their internal–external shape. We experimentally identified the copper binding site, aptamotif, and highlighted its importance in G–C pairs using sequence mutation and deletion analysis. The potential aptamotif in the high affinity copper binding aptamer (Cu-A2) was predicted to be in 5 G–C pairs and an A–G bridge. The mutation and deletion analysis shows that the high G–C pairing patterns and short stem-interval distance play important roles in the copper binding. The understanding of the binding interaction of copper with the aptamotif would give an insight into the mode of interaction and its possible mechanism of G–C pair remodelling in the aptamer structure. We have also developed an Aptamer Integrated Recovery Platform (AIRP) for copper using a specific aptamer, Cu-A2. Biotinylated Cu-A2 was conjugated on the streptavidin agarose resin and applied to copper solutions. The AIRP proposed by us has the following advantages:

• Cu-A2 on AIRP retained its bioactivity and recovered more than 99% of copper from aqueous solutions.

• AIRP was not susceptible to low pH and the presence of other metal ions.

• AIRP shows high reusability of more than 20 times (under laboratory conditions) and without discernible loss in copper capturing activity.

• The AIRP has been used on the local mine drainage samples with high recovery efficiency and specificity.

• Repeatable copper retrieval by system regeneration and copper-risk assessment.

Unlike other affinity reagents, aptamers can undergo multiple cycles of denaturation and regeneration so this allows our AIRP to be recyclable, reusable and economic. The results suggest that the copper recovery by AIRP can be a major component in the renewable energy system and its potential application as a biosensor may help to minimize the environmental impacts of mining including erosion, and contamination of water and soil. To the best of our knowledge, this is the first study to demonstrate the copper recovery by using an aptamer integrated system and can be used as a selective metal enrichment method in high value-added material processing.

Acknowledgements

Simranjeet Singh Sekhon and Sang-Hee Lee contributed equally to this work. This study was performed by the support of the "Cooperative Research Program for Agriculture Science & Technology Development (Project No. PJ012568)" (Rural Development Administration, Republic of Korea). This work was also supported by the National Research Foundation of Korea (NRF) grant funded by the Ministry of Science, ICT & Future Planning (NRF-2015R1A4A1041869). The authors are grateful for their support.

References

1 M. Pasta, C. D. Wessells, R. A. Huggins and Y. Cui, *Nat. Commun.*, 2012, **3**, 1149.
2 E. L. Watkin, S. E. Keeling, F. A. Perrot, D. W. Shiers, M. L. Palmer and H. R. Watling, *J. Ind. Microbiol. Biotechnol.*, 2009, **36**, 461–465.
3 E. Islam, X. E. Yang, Z. L. He and Q. Mahmood, *J. Zhejiang Univ., Sci., B*, 2007, **8**, 1–13.
4 L. S. Jelaska, M. Blanusa, P. Durbesic and S. D. Jelaska, *Ecotoxicol. Environ. Saf.*, 2007, **66**, 74–81.
5 M. A. Hossain, H. H. Ngo, W. S. Guo and T. Setiadi, *Bioresour. Technol.*, 2012, **121**, 386–395.
6 F. Tisato, C. Marzano, M. Porchia, M. Pellei and C. Santini, *Med. Res. Rev.*, 2010, **30**, 708–749.
7 A. R. White, G. Multhaup, D. Galatis, W. J. McKinstry, M. W. Parker, R. Pipkorn, K. Beyreuther, C. L. Masters and R. Cappai, *J. Neurosci.*, 2002, **22**, 365–376.
8 A. Kunhikrishnan, N. S. Bolan, R. Naidu and W. I. Kim, *J. Hazard. Mater.*, 2013, **261**, 784–792.
9 K. Murase, K.-I. Machida and G.-Y. Adachi, *J. Alloys Compd.*, 1995, **217**, 218–225.
10 S. Chakravarty, S. Pimple, H. T. Chaturvedi, S. Singh and K. K. Gupta, *J. Hazard. Mater.*, 2008, **159**, 396–403.
11 A. Troupis, A. Hiskia and E. Papaconstantinou, *Environ. Sci. Technol.*, 2002, **36**, 5355–5362.
12 H. Aydin, Y. Bulut and C. Yerlikaya, *J. Environ. Manage.*, 2008, **87**, 37–45.
13 B. Yu, Y. Zhang, A. Shukla, S. S. Shukla and K. L. Dorris, *J. Hazard. Mater.*, 2000, **80**, 33–42.
14 S. S. Sekhon, S. G. Kim, S. H. Lee, A. Jang, J. Min, J. Y. Ahn and Y. H. Kim, *Mol. Cell. Toxicol.*, 2013, **9**, 311–317.
15 S. E. Kim, K. Y. Ahn, J. S. Park, K. R. Kim, K. E. Lee, S. S. Han and J. Lee, *Anal. Chem.*, 2011, **83**, 5834–5843.
16 K. Han, Z. Liang and N. Zhou, *Sensors*, 2010, **10**, 4541–4557.
17 W. Zhou, P. J. Huang, J. Ding and J. Liu, *Analyst*, 2014, **139**, 2627–2640.
18 H. J. Um, M. Kim, S. H. Lee and Y. H. Kim, *AIDS*, 2012, **26**, 1599–1605.
19 A. K. Cheng, D. Sen and H. Z. Yu, *Bioelectrochemistry*, 2009, **77**, 1–12.
20 J. Y. Ahn, E. Kim, J. Kang and S. Kim, *Nucleic Acid Ther.*, 2011, **21**, 179–183.
21 J. Y. Ahn, S. W. Lee, H. S. Kang, M. Jo, D. K. Lee, T. Laurell and S. Kim, *J. Proteome Res.*, 2010, **9**, 5568–5573.
22 Y. Ohno, K. Maehashi and K. Matsumoto, *J. Am. Chem. Soc.*, 2010, **132**, 18012–18013.
23 K. Urmann, J. G. Walter, T. Scheper and E. Segal, *Anal. Chem.*, 2015, **87**, 1999–2006.
24 W. Zhao, W. Chiuman, M. A. Brook and Y. Li, *ChemBioChem*, 2007, **8**, 727–731.

25 Z. Huang and J. W. Szostak, *RNA*, 2003, **9**, 1456–1463.
26 S. B. Long, M. B. Long, R. R. White and B. A. Sullenger, *RNA*, 2008, **14**, 2504–2512.
27 J. Hoinka, E. Zotenko, A. Friedman, Z. E. Sauna and T. M. Przytycka, *Bioinformatics*, 2012, **28**, i215–i223.
28 Y. S. Kim, J. H. Niazi and M. B. Gu, *Anal. Chim. Acta*, 2009, **634**, 250–254.
29 M. Zuker, *Nucleic Acids Res.*, 2003, **31**, 3406–3415.
30 C. M. Neculita, G. J. Zagury and B. Bussiere, *J. Environ. Qual.*, 2007, **36**, 1–16.
31 K. A. Lee, J. Y. Ahn, S. H. Lee, S. Singh Sekhon, D. G. Kim, J. Min and Y. H. Kim, *Sci. Rep.*, 2015, **5**, 10897.
32 S. K. Sharma, P. J. Rogler and K. D. Karlin, *J. Porphyrins Phthalocyanines*, 2015, **19**, 352–360.
33 M. Sundaralingam and J. A. Carrabine, *J. Mol. Biol.*, 1971, **61**, 287–309.
34 S. Itoh, H. W. Kim, O. Nakagawa, K. Ozumi, S. M. Lessner, H. Aoki, K. Akram, R. D. McKinney, M. Ushio-Fukai and T. Fukai, *J. Biol. Chem.*, 2008, **283**, 9157–9167.
35 Y. Li, Z. Y. Yang and T. R. Li, *Chem. Pharm. Bull.*, 2008, **56**, 1528–1534.
36 J. L. Sagripanti, P. L. Goering and A. Lamanna, *Toxicol. Appl. Pharmacol.*, 1991, **110**, 477–485.
37 J. Y. Choi, D. S. Kim and J. Y. Lim, *J. Environ. Sci. Health, Part A: Toxic/Hazard. Subst. Environ. Eng.*, 2006, **41**, 1155–1172.
38 D. T. Sponza and O. Gok, *Water Sci. Technol.*, 2011, **64**, 2282–2292.
39 K. H. Lin, H. T. Hsu, Y. W. Ko, Z. X. Shieh and H. L. Chiang, *J. Hazard. Mater.*, 2009, **171**, 208–214.
40 V. Stergar, J. Zagorc-Koncan and A. Zgajnar-Gotvanj, *Water Sci. Technol.*, 2003, **48**, 97–102.
41 J. R. Hunt and H. Zeng, *Am. J. Clin. Nutr.*, 2004, **80**, 924–931.
42 C. E. Hajdin, F. Ding, N. V. Dokholyan and K. M. Weeks, *RNA*, 2010, **16**, 1340–1349.
43 R. An, Y. Jia, B. Wan, Y. Zhang, P. Dong, J. Li and X. Liang, *PLoS One*, 2014, **9**, e115950.

